Drug Design, Development and Therapy

Dovepress
Taylor & Francis Group

Open Access Full Text Article

ORIGINAL RESEARCH

Comprehensive Bioactive Compound Profiling of *Artocarpus heterophyllus* Leaves: LC-MS/MS Analysis, Antioxidant Potential, and Molecular Insights

Lelly Yuniarti[1], Taufik Muhammad Fakih[2], Maya Tejasari[3], Raden Anita Indriyanti[4], Erni Maryam[5], Bambang Hernawan Nugroho[6]

[1]Department of Biochemistry, Faculty of Medicine, Universitas Islam Bandung, Jl. Tamansari, Bandung, 40116, Indonesia; [2]Department of Pharmacy, Faculty of Mathematics and Natural Sciences, Universitas Islam Bandung, Jl. Ranggagading, Bandung, 40116, Indonesia; [3]Department of Histology, Faculty of Medicine, Universitas Islam Bandung, Jl. Tamansari, Bandung, 40116, Indonesia; [4]Department of Pharmacology, Faculty of Medicine, Universitas Islam Bandung, Jl. Tamansari, Bandung, 40116, Indonesia; [5]Study Program in Skin Aging and Medical Aesthetics, Faculty of Medicine, Universitas Jenderal Achmad Yani, Jl. Terusan Jenderal Sudirman, Cimahi, 40531, Indonesia; [6]Department of Pharmacy, Faculty of Mathematics and Natural Sciences, Universitas Islam Indonesia, Jl. Kaliurang, Sleman, 55584, Indonesia

Correspondence: Lelly Yuniarti, Department of Biochemistry, Faculty of Medicine, Universitas Islam Bandung, Jl. Tamansari, Bandung, 40116, Indonesia, Tel +62 813-2008-6300, Email lelly.yuniarti@gmail.com

Purpose: *Artocarpus heterophyllus* leaves, rich in phytochemicals, present a promising source of natural bioactive compounds for therapeutic and cosmetic applications. This study evaluated the phytochemical composition, antioxidant potential, and tyrosinase inhibition activities of leaf extracts while assessing the enzyme inhibition properties of key compounds through molecular docking and dynamics simulations.

Patients and Methods: Ethanol and ethyl acetate extracts were analyzed using Thin Layer Chromatography (TLC) and Liquid Chromatography-Mass Spectrometry/Mass Spectrometry (LC-MS/MS). Antioxidant activity was determined via DPPH radical scavenging and tyrosinase inhibition was compared against kojic acid. Molecular docking and molecular dynamics simulations explored binding interactions of Artocarpin and Sitosterol with matrix metalloproteinases (MMPs) and tyrosinase.

Results: Artocarpin and Sitosterol were identified as primary bioactive compounds. Ethanol extracts exhibited stronger tyrosinase inhibition (IC_{50}: 177.24 ppm), while ethyl acetate extracts showed superior antioxidant activity (IC_{50}: 117.64 ppm). Molecular docking highlighted high binding affinities of Artocarpin and Sitosterol with MMP-13 and tyrosinase. MD simulations confirmed stable interactions, particularly between Artocarpin and MMP-13, supporting its potential as a therapeutic agent.

Conclusion: Artocarpin and Sitosterol from *Artocarpus heterophyllus* leaf extracts demonstrate potent antioxidant, enzyme inhibitory, and tyrosinase inhibition activities. These findings underscore their potential for managing oxidative stress, inflammation, and pigmentation disorders, warranting further investigation into their bioavailability and formulation for therapeutic and cosmetic uses.

Keywords: *Artocarpus heterophyllus*, bioactive compound profiling, antioxidant activity, tyrosinase inhibition, computational study

Introduction

Medicinal plants play a crucial role in the development of pharmaceutical and cosmetic products, serving as a rich source of bioactive compounds. These natural compounds, including flavonoids, terpenoids, and phenolic acids, are known for their potent antioxidant and anti-inflammatory properties.[1,2] Flavonoids, as one of the largest groups of polyphenolic compounds, have been extensively studied for their ability to scavenge free radicals and regulate oxidative stress. Oxidative stress occurs when an imbalance between free radical production and antioxidant defenses leads to cellular damage, lipid peroxidation, and inflammation.[3] This condition is a major contributor to chronic diseases such as cancer, cardiovascular disorders, and neurodegenerative diseases.[4] Antioxidant compounds from plants have been shown to mitigate these effects by enhancing the body's endogenous defense systems.[5] Moreover, flavonoids and terpenoids are

Received: 20 November 2024
Accepted: 6 February 2025
Published: 18 February 2025

increasingly recognized for their enzyme inhibitory properties, offering therapeutic potential against various pathophysiological processes.[6,7] These attributes highlight the significance of exploring phytochemicals for their pharmacological and cosmetic applications.

Artocarpus heterophyllus, commonly known as jackfruit, is a tropical plant that has been traditionally used for its nutritional and medicinal properties. Various parts of the plant, particularly its leaves, have been utilized in treating skin disorders, inflammation, and oxidative stress-related conditions.[8,9] The leaves of *Artocarpus heterophyllus* are rich in flavonoids and terpenoids, which are bioactive compounds with diverse therapeutic benefits. Research has shown that these compounds exhibit antioxidant and anti-inflammatory activities, supporting the traditional use of the plant in addressing oxidative stress.[10] Furthermore, terpenoids and phenolic acids found in the leaves are associated with regulating key enzymes involved in inflammation and tissue remodeling. In addition to their therapeutic roles, *Artocarpus heterophyllus* extracts have potential applications in cosmetics, particularly in controlling pigmentation and improving skin health.[11,12] The plant's ability to address both health and cosmetic concerns underscores its versatility as a natural remedy. Exploring the phytochemical composition of *Artocarpus heterophyllus* leaves is essential to understanding their bioactive potential.[13]

This study focuses on analyzing the bioactive compounds present in *Artocarpus heterophyllus* leaf extracts obtained using ethyl acetate and ethanol solvents. The choice of these solvents is based on their polarity, which influences the range and efficiency of compound extraction. Techniques such as Thin Layer Chromatography (TLC) and Liquid Chromatography-Mass Spectrometry/Mass Spectrometry (LC-MS/MS) were employed to identify and characterize the major compounds in the extracts. The antioxidant activity of the extracts was evaluated to assess their potential in mitigating oxidative stress, a key factor in chronic diseases and aging.[14] Additionally, the tyrosinase inhibitory activity of the extracts was studied for its relevance in cosmetic applications, particularly in skin pigmentation control.[15,16] The study also explores the correlation between the chemical profiles of the extracts and their observed bioactivities. By understanding these properties, the research seeks to highlight the therapeutic and cosmetic applications of *Artocarpus heterophyllus* extracts. These findings are expected to provide insights into the plant's potential as a source of natural bioactive compounds.

By integrating traditional knowledge with scientific research, this study aims to establish the significance of *Artocarpus heterophyllus* leaf extracts in health and skincare. The investigation highlights the role of solvent selection in optimizing the extraction of bioactive compounds. The study's focus on antioxidant and tyrosinase inhibitory activities aligns with current trends in developing natural alternatives for therapeutic and cosmetic applications. These efforts contribute to the growing interest in plant-based solutions for managing oxidative stress and pigmentation-related concerns.[17,18] *Artocarpus heterophyllus*, with its rich phytochemical profile, emerges as a promising candidate for further exploration in these fields. Utilizing advanced analytical techniques, including LC-MS/MS, molecular docking, and molecular dynamics (MD) simulations, the study provides a comprehensive understanding of the phytochemical composition and its bioactivities. These findings not only validate the ethnopharmacological uses of *Artocarpus heterophyllus* but also support its relevance in modern therapeutic and cosmetic innovations (Video S1). Future research will focus on clinical evaluations and optimizing formulations to enhance bioavailability and efficacy, paving the way for its integration into health and skincare solutions.

Material and Methods

General

TLC analyses were conducted using 20×20 cm aluminum sheets coated with silica gel 60 F_{254} (Sigma-Aldrich, St. Louis, USA) and 0.25 mm silica gel G-25 UV_{254} pre-coated glass TLC plates (Sigma-Aldrich, St. Louis, USA), suitable for both vacuum column chromatography and preparative TLC procedures. Terpenoids and steroids were visualized on TLC plates by applying Liebermann-Burchard reagent as a staining agent. For compound profiling, a UHPLC Vanquish system coupled with a Q Exactive Plus Orbitrap High-Resolution Mass Spectrometer (Thermo Scientific, Waltham, MA, USA) was used to perform LC-MS/MS analysis. NMR data were collected using a Bruker Avance III™ HD 600 MHz NMR spectrometer (Bruker BioSpin GmbH, Rheinstetten, Germany), with ^1H spectra recorded at 500 MHz and ^13C spectra at 150 MHz, using TMS as the reference standard in deuterated chloroform, and chemical shifts reported in δ (ppm). Antioxidant testing utilized DPPH radical scavenging assays, where a microplate reader recorded absorbance at 517 nm. The assay was performed in 70% ethanol, with Trolox as the standard, and results were reported as μmol Trolox

equivalents (TE) per gram of sample. For the tyrosinase inhibition assay, absorbance was measured at 475 nm using a multi-well plate reader. Solutions were prepared with L-DOPA in a 50 mM phosphate buffer (pH 6.8), and kojic acid was used as a positive control for reference in evaluating enzyme inhibition activity.

Plant Material

The *Artocarpus heterophyllus* leaves were collected from Kota Bandung, West Java, Indonesia, in August 2024. The plant specimen was formally identified and authenticated at the Herbarium Bandungense, housed within the School of Life Sciences and Technology, Bandung Institute of Technology. The identification process was completed under voucher number 8366/IT1. C11.2/TA.00/2024, and the specimen was subsequently deposited in the herbarium's collection for documentation and future reference. The identification and deposition process were officially validated by the Deputy Dean of Resources, Angga Dwiartama, S.Si., M.Si., Ph.D., ensuring the credibility and accuracy of the botanical identification.

Extraction and Isolation

The leaves of *Artocarpus heterophyllus* (1.6 kg) were extracted using the maceration method with ethyl acetate (16 L) as the solvent over a period of 3–5 days. The resulting filtrate was evaporated to yield a viscous ethyl acetate extract, with a total weight of 6.078 g for batch 1 and 25.573 g for batch 2. This extract was then monitored using Thin Layer Chromatography (TLC) to confirm the presence of the desired compounds. Additionally, a separate extraction was performed using ethanol as the solvent. A total of 1 kg of *Artocarpus heterophyllus* leaves was extracted in 10 L of ethanol using the maceration method for 3–5 days. The ethanol filtrate was evaporated to yield a viscous ethanolic extract, resulting in 15.8 g for batch 1 and 26.4579 g for batch 2. This ethanolic extract was also monitored using TLC to identify the compound components. TLC monitoring revealed several fractions with specific Rf patterns, which were further isolated. The identified compounds exhibited distinct characteristics in TLC, suggesting the presence of compound groups such as flavonoids, phenolic acids, and terpenoids/steroids.[19,20] In the ethyl acetate extract, a fraction with a specific Rf value of 0.52 (brown color with sulfuric acid-methanol) was identified and collected as a colorless powder. In the ethanol extract, a fraction with an Rf value of approximately 0.48 (brown color with sulfuric acid-methanol) was isolated and collected in the form of a colorless powder. All isolated compounds from both extracts were further analyzed using LC-MS/MS for further characterization.

LC-MS/MS Analysis

Each isolated compound (1 mg) was dissolved in 1 mL of methanol (LC-MS grade, Chromasolv®). A 1-microliter *Artocarpus heterophyllus* leaves extract aliquot was injected into the column. A gradient elution was performed using 0.1% formic acid (v/v) in water alongside acetonitrile with 0.1% formic acid (v/v), starting with a ratio of 95:5, shifting to 60:40 from 1.00 to 8.00 minutes, then 0:100 from 8.00 to 13.00 minutes, and concluding with 95:5. The flow rate was maintained at 0.3 mL/min. Instrument settings included: acquisition time of 0.00–16.00 minutes, mass range of 50.00–1200.00 m/z, scan interval of 0.100 s, low CE of 6 eV, high CE ranging from 10–40 eV, cone voltage at 30 V, collision energy at 6 eV, acquisition mode ESI (+), capillary voltage at 2 kV, source temperature set to 120 °C, desolvation temperature at 500 °C, cone gas flow at 50 L/h, desolvation gas flow at 1000 L/h, sample temperature set to 20 °C, and column temperature at 40 °C.[21] Data were processed with UNIFI software (version 1.8, Waters Corporation, Milford, MA, USA), utilizing a screening solution workflow to facilitate automated data handling and positive identifications.[22] The results were compared against a database containing over 1200 compounds, cross-referenced by chemical structure, molecular formula, and molecular weight from multiple online resources.

Multi Targeted Molecular Docking Study

For the molecular docking analysis, various crystal structures were utilized, including human tyrosinase-related protein 1 (PDB ID: 5M8Q), Melanocyte Inducing Transcription Factor (MITF) (PDB ID: 5T3Q), Matrix Metalloproteinase-1 (MMP-1, PDB ID: 1HFC), Matrix Metalloproteinase-2 (MMP-2, PDB ID: 1HOV), Matrix Metalloproteinase-8 (MMP-8, PDB ID: 5H8X), Matrix Metalloproteinase-9 (MMP-9, PDB ID: 2OW1), Matrix Metalloproteinase-13 (MMP-13, PDB ID: 2OZR), TGF-Beta receptor type 1 kinase (PDB ID: 6B8Y), fibroblast collagenase (PDB ID: 1CGL), and elastase (PDB ID: 3HGP).[23–31] The selected

receptor crystal structures were chosen based on their roles in oxidative stress, inflammation, and pigmentation-related disorders, aligning with the bioactivities of the tested compounds. Proteins underwent refinement via the Protein Preparation Wizard in Schrödinger's Maestro 2020–3 software (Schrödinger, New York, NY, USA), where missing hydrogens were added, and partial charges were assigned using the OPLS_2005 (Optimized Potentials for Liquid Simulations 2005) forcefield.[32,33] Proteins were prepped in a restrained minimization state with hydrogens and heavy atoms. The 2D chemical structures of compounds from *Artocarpus heterophyllus* leaves extract, identified through LC-MS/MS, were converted into 3D forms using the LigPrep Module in Maestro Schrödinger 2020–3 with OPLS_2005, adjusting pH to 7.4 through Epik. LigPrep ensured appropriate protonation states, tautomeric forms, and ionization, with bond orders validated for accuracy. To define the docking region, the grid box was aligned by selecting the native ligand from the protease receptor to centralize docked compounds within the same spatial dimensions as the binding region. The docking procedure was performed in extra precision (XP) mode through Glide, applying the OPLS_2005 forcefield under flexible ligand and fixed receptor parameters. Each ligand's efficacy as a receptor inhibitor was assessed by scoring docked poses using the Molecular Mechanics-Generalized Born Surface Area (MM-GBSA) methodology.[34]

Multi Targeted Molecular Dynamics Simulation

GROMACS 2024.4 was utilized to perform molecular dynamics (MD) simulations on the protein-Artocarpin and protein-Sitosterol complexes, each simulated over 50 ns.[35,36] A dodecahedral unit cell was defined with a 1 nm buffer between the protein surface and box edge, solvated using the Simple Point Charge (SPC) water model. The CHARMM36 (Chemistry at HARvard Macromolecular Mechanics 36) was selected for target topologies, and the system underwent energy minimization with the steepest descent integrator for 50,000 steps, targeting a force convergence threshold of 1000 kcal/mol/nm.[37] Following this, each protein-ligand complex was equilibrated under both NVT (constant number of particles, volume, and temperature) and NPT (constant number of particles, pressure, and temperature) conditions for 1000 ps, with temperature and pressure stabilization set to 300 K and 1 bar using the Berendsen thermostat and Parrinello-Rahman barostat, respectively. MD simulations were conducted for 50 ns with coordinate snapshots saved every 2 fs, balancing between runtime efficiency and data capture. The stability observed in fluctuation graphs confirmed successful equilibration. GROMACS analytical tools were employed for structural and conformational analyses across systems, while MM-PBSA (Molecular Mechanics-Poisson Boltzmann Surface Area) calculations were used to estimate binding free energies from the snapshots.[38]

DPPH Radical Scavenging Activity

The DPPH radical scavenging activity was assessed by combining 100 µL of the *Artocarpus heterophyllus* leaves extract with 100 µL of DPPH solution (0.1 mM in 70% ethanol) and incubating the mixture in the dark at 25–27 °C for 30 minutes. Distilled water was used as a control and as a substitute for the sample. Absorbance was measured at 517 nm using a microplate reader, and scavenging activity was calculated as follows: Scavenging activity (%) = $[(A_{control} - A_{sample}) / A_{control}] \times 100$, where $A_{control}$ is the absorbance of the DPPH solution alone, and A_{sample} is the absorbance of the sample mixed with DPPH.[39] The activity was reported as IC_{50}, representing the concentration of the sample needed to inhibit 50% of the initial DPPH concentration. The IC_{50} value was obtained from a linear regression graph, and results were expressed in µmol Trolox equivalents (TE) per gram of sample for each fraction tested.

Tyrosinase Enzyme Inhibitory Activity

The tyrosinase inhibition activity of *Artocarpus heterophyllus* leaves extract was determined by preparing a reaction mixture in a multi-well plate. A 3.2 mM L-DOPA solution in 50 mM phosphate buffer (pH 6.8) was prepared. Then, 10 µL of various concentrations of *Artocarpus heterophyllus* leaves extract was diluted with 40 µL of 50 mM K_3PO_4 buffer (pH 6.8) and combined with 70 µL of tyrosinase solution (150 units/mL). This mixture was incubated for 10 minutes. Afterward, 80 µL of the L-DOPA solution (3.2 mM) was added to each well and left to incubate for another 10 minutes. The absorbance was read at 475 nm using a multi-well plate reader. Kojic acid was used as a positive control to benchmark inhibition. Tyrosinase inhibition activity was calculated with the following formula: Tyrosinase inhibitory activity (%) = $\{[A_{control} - (A_{sample} - A_{colour})] / (A_{control} - A_{blank})\} \times 100$, where A_{blank} is the absorbance of deionized water, A_{colour} is the absorbance of the sample mixed with phosphate

buffer, $A_{control}$ represents the absorbance of the buffer-tyrosinase-L-DOPA mixture without the sample, and A_{sample} is the absorbance from the reaction solution.[40] The IC_{50} values were calculated similarly to those in the DPPH analysis.

Results

Extraction of Artocarpus Heterophyllus Leaves

The extraction of *Artocarpus heterophyllus* leaves using ethyl acetate and ethanol through maceration yielded different concentrations of bioactive compounds. Ethyl acetate extraction produced 0.38% yield (6.078 g from 1.6 kg of leaves), while ethanol extraction achieved a higher yield of 1.58% (15.8 g from 1 kg of leaves). Thin Layer Chromatography (TLC) and LC-MS/MS analyses revealed that both extracts were dominated by flavonoids and terpenoids/steroids, though in varying proportions. Flavonoids constituted 50% of the ethyl acetate extract and 35% of the ethanol extract, while terpenoids/steroids made up 25% and 30%, respectively (Figure 1). Phenolic acids were also present in moderate amounts, with a slightly higher concentration in the ethanol extract. Hydrocarbons and other compounds appeared in minimal quantities across both extracts, indicating that the primary components were flavonoids and terpenoids/steroids. These findings underscore the selective extraction capabilities of ethyl acetate and ethanol, emphasizing the influence of solvent polarity. Both extracts thus show a high potential for yielding bioactive compounds, with ethanol demonstrating a broader range of extractable compounds.

The prominent presence of flavonoids and terpenoids/steroids in both ethyl acetate and ethanol extracts suggests significant potential for isolating these bioactive compounds from *Artocarpus heterophyllus* leaves. Flavonoids are widely known for their antioxidant properties, while terpenoids and steroids have various therapeutic applications, highlighting the extracts' value in pharmaceutical contexts. This study recommends using liquid-liquid extraction with solvents of varying polarity, such as n-hexane and water, to further enhance isolation of these compounds by optimizing selectivity based on solubility. Such targeted extraction methods may yield purer fractions, allowing for more effective pharmacological studies on individual compounds. Additionally, the presence of phenolic acids, although moderate,

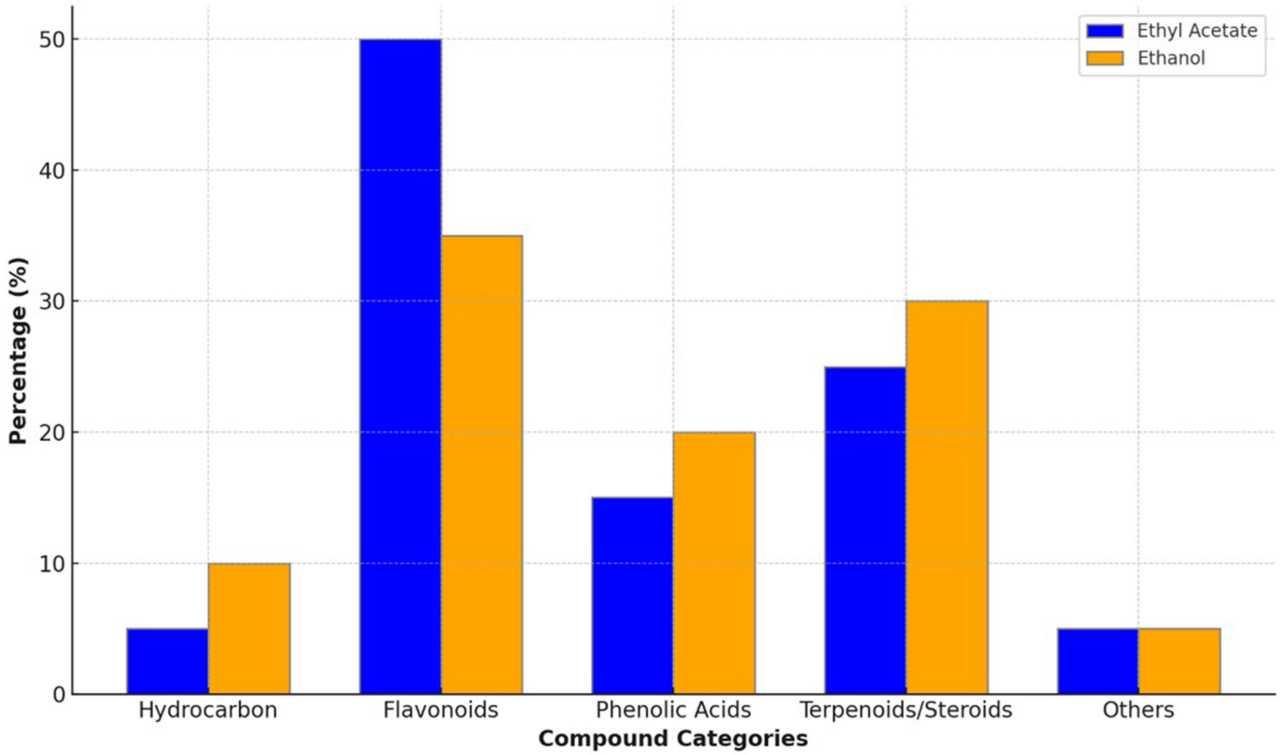

Figure 1 Percentage composition of compound categories in ethyl acetate and ethanol extracts of *Artocarpus heterophyllus* leaves.

https://doi.org/10.2147/DDDT.S507658

contributes to the overall antioxidant potential of the extracts.[41,42] These results emphasize the leaves of *Artocarpus heterophyllus* as a viable source of beneficial phytochemicals, particularly flavonoids and terpenoids.

Isolation and LC-MS/MS Identification From Isolates of Artocarpus Heterophyllus Leaves

The ethyl acetate and ethanol extracts of *Artocarpus heterophyllus* leaves were analyzed to identify their compound composition, focusing on key compounds based on retention time, molecular mass, and molecular formula (Table 1, Figure 2). In the ethyl acetate extract, Cintramide emerged as the most abundant compound, comprising 46.61% of the extract at a retention time of 7.48 minutes, indicating its strong affinity for ethyl acetate. Other significant compounds included Licoflavone C and 3,4,5-trimethoxy cinnamic acid, with compositions of 19.14% and 10.53%, respectively.

Table 1 Compounds Identified by LC-MS/MS From the Isolates of Artocarpus Heterophyllus Ethyl Acetate and Ethanol Extracts

No	Retention Time	Calculated Mass (m/z)	Molecular Weight	Molecular Formula	Prediction Compound	Composition Percentage (%)
Ethyl acetate extract of *Artocarpus heterophyllus* leaves						
1	3.81	339.1051	338.35	$C_{20}H_{18}O_5$	Licoflavone c	19.14
2	4.40	281.0674	280.23	$C_{13}H_{12}O_7$	2-{[3-(4-hydroxyphenyl)prop-2-enoyl]oxy}butanedioic acid	11.74
3	4.88	415.2087	414.71	$C_{29}H_{50}O$	Sitosterol	1.55
4	5.27	437.2387	436.18	$C_{26}H_{28}O_6$	Artocarpin	0.95
5	5.63	407.2061	406.47	$C_{25}H_{26}O_5$	Cycloaltilisin 7	0.77
6	5.85	353.1235	354.11	$C_{20}H_{18}O_6$	Artocarpesin	0.61
7	6.20	333.0979	332.31	$C_{17}H_{16}O_7$	5,7-dihydroxy-2-(2-hydroxy-4,6-dimethoxyphenyl)-2,3-dihydro-1-benzopyran-4-one	4.84
8	6.58	225.0767	192.21	$C_{11}H_{12}O_3$	Vanillylidene acetone	3.25
9	7.48	238.1083	237.25	$C_{12}H_{15}NO_4$	Cintramide	46.61
10	8.38	239.0929	238.24	$C_{12}H_{14}O_5$	3,4,5-trimethoxy cinnamic acid	10.53
Ethanol extract of *Artocarpus heterophyllus* leaves						
1	3.83	339.1048	338.35	$C_{20}H_{18}O_5$	Licoflavone C	14.57
2	4.51	377.1494	376.36	$C_{16}H_{24}O_{10}$	2-{[1,3-dihydroxy-1-(4-hydroxy-3-methoxyphenyl) propan-2-yl]oxy}-6-(hydroxymethyl)oxane-3,4,5-triol	2.25
3	4.75	303.0891	302.28	$C_{16}H_{14}O_6$	Artocarpanone	2.99
4	4.90	279.0879	278.26	$C_{14}H_{14}O_6$	[7-hydroxy-4-oxo-2-(2-oxopropyl)-2,3-dihydro-1-benzopyran-5-yl]acetic acid	2.31
5	5.08	349.0923	348.30	$C_{17}H_{16}O_8$	Asterric acid	3.55
6	5.65	407.2061	406.47	$C_{25}H_{26}O_5$	Cycloaltilisin 7	0.93
7	6.20	333.0979	332.31	$C_{17}H_{16}O_7$	5,7-dihydroxy-2-(2-hydroxy-4,6-dimethoxyphenyl)-2,3-dihydro-1-benzopyran-4-one	7.35
8	7.21	237.0775	236.22	$C_{12}H_{12}O_5$	7-(2-hydroxyethoxy)-6-methoxychromen-2-one	0.32
9	7.32	223.0974	222.24	$C_{12}H_{14}O_4$	Ethyl ferulate	0.76
10	7.59	441.1544	440.44	$C_{24}H_{24}O_8$	(6r)-9,11-dihydroxy-2,3,6-trimethoxy-8-(3-methylbut-2-en-1-yl)-6h-5,7-dioxatetraphen-12-one	4.94
11	8.35	239.0929	238.24	$C_{12}H_{14}O_5$	2s)-3-{[2-(4-hydroxyphenyl)acetyl]oxy}-2-methylpropanoic acid	8.48
12	8.79	458.1816	457.44	$C_{20}H_{23}N_7O_6$	(2s)-2-[(4-{1-hydroxy-3-imino-4h,5h,6h,6ah,7h,9h-imidazo[1,5-f]pteridin-8-yl}phenyl)formamido]pentanedioic acid	44.14
13	9.91	369.0971	368.34	$C_{20}H_{16}O_7$	3-[4-(acetyloxy)phenyl]-7-methoxy-4-oxochromen-5-yl acetate	7.40

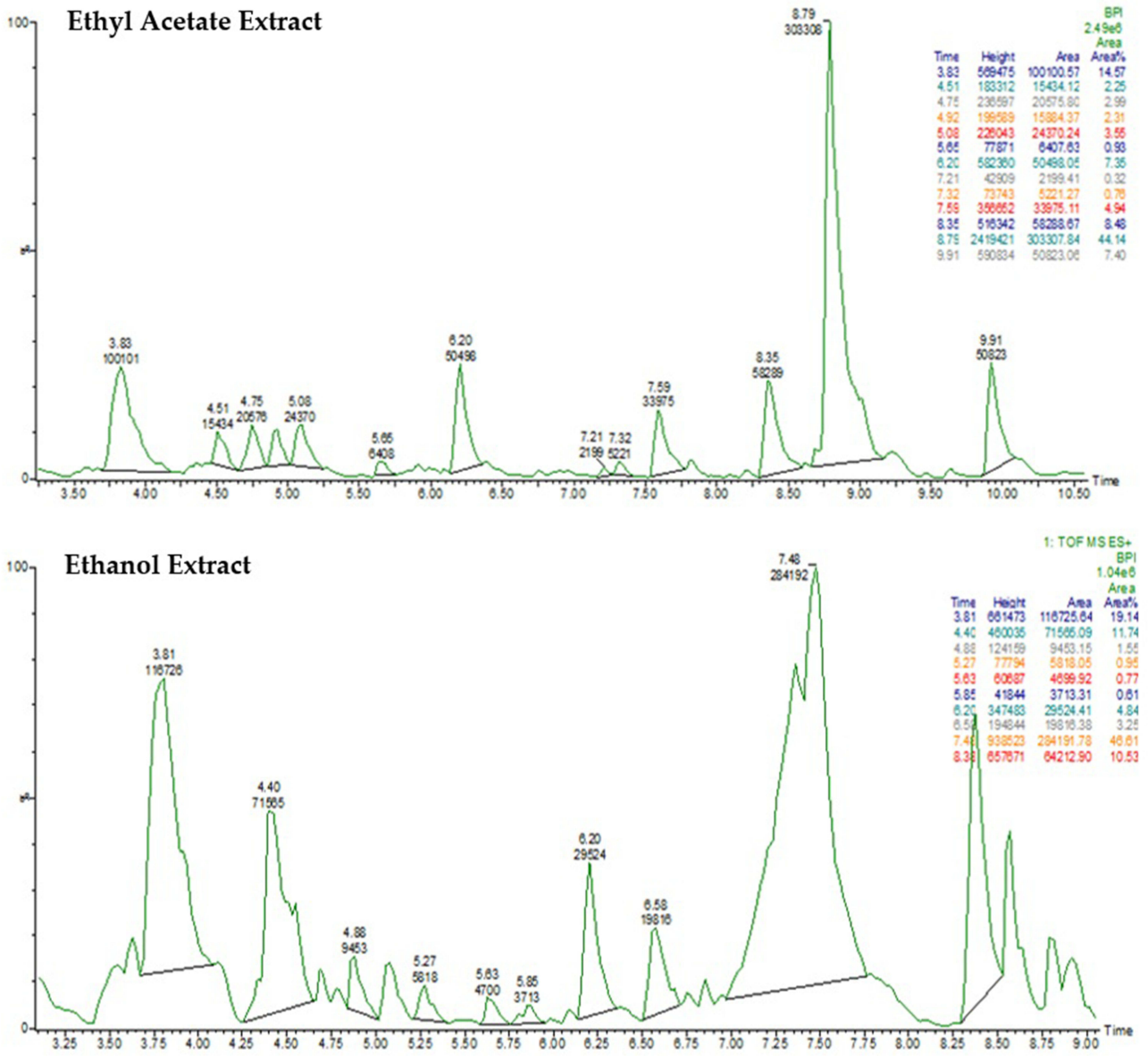

Figure 2 LC-MS/MS chromatogram of compounds identified from the isolates of *Artocarpus heterophyllus* ethyl acetate and ethanol extracts.

These compounds, especially flavonoids and cinnamic acid derivatives, are notable for their antioxidant and anti-inflammatory properties, which suggest that the ethyl acetate extract may possess significant bioactivity. The presence of smaller amounts of compounds like Sitosterol and Artocarpin, though less abundant, adds to the diverse composition of the extract. Each of these compounds was carefully identified using TLC and LC-MS/MS, ensuring accurate classification. The predominance of these bioactive molecules in the ethyl acetate extract makes it a valuable source for further isolation studies.

In contrast, the ethanol extract exhibited a unique chemical profile with several complex compounds that differed from those found in the ethyl acetate extract. The primary compound in the ethanol extract was (2s)-2-[(4-{1-hydroxy-3-imino-4h,5h,6h,6ah,7h,9h-imidazo[1,5-f]pteridin-8-yl}phenyl)formamido]pentanedioic acid, accounting for 44.14% of the total composition and detected at a retention time of 8.79 minutes. This compound's presence in high concentration underscores the ethanol extract's potential for therapeutic applications, particularly due to the bioactive properties often associated with such structures. Other prominent compounds included Licoflavone C (14.57%) and (2s)-3-{[2-(4-hydroxyphenyl)acetyl]oxy}-2-methylpropanoic acid (8.48%), which contribute to the extract's diversity. Smaller amounts of compounds, such as

https://doi.org/10.2147/DDDT.S507658

Asterric acid and Artocarpanone, added further complexity to the extract's profile, indicating a wide range of potential bioactivities. The varied composition of the ethanol extract suggests a strong potential for therapeutic use.

In addition, the differences between the ethyl acetate and ethanol extracts highlight the influence of solvent choice on extraction efficiency and compound profile.[43,44] Ethyl acetate appears to be more effective at extracting simple bioactive compounds, with Cintramide, Licoflavone C, and cinnamic acid derivatives making up the bulk of the extract. Meanwhile, ethanol effectively extracted larger, more complex molecules such as (2s)-2-[(4-{1-hydroxy-3-imino-4h,5h,6h,6ah,7h,9h-imidazo[1,5-f]pteridin-8-yl}phenyl)formamido]pentanedioic acid, along with other unique flavonoids and phenolic compounds. These differences in compound profiles suggest that both extracts hold promise for various therapeutic applications, with ethyl acetate potentially targeting antioxidant and anti-inflammatory effects, while ethanol may focus on more complex pharmacological activities. Both extracts' bioactive potential, especially as natural sources of antioxidants and therapeutic agents.

Multi Targeted Molecular Docking Study

The molecular docking simulations of compounds identified from *Artocarpus heterophyllus* extracts provide valuable insights into their potential as enzyme inhibitors targeting fibroblast collagenase, elastase, MITF, MMP-1, and MMP-2. Table 2 reveals that several compounds, particularly Cycloaltilisin 7 and Sitosterol, exhibited strong binding affinities with low MMGBSA binding energies, suggesting stable interactions with these enzymes. Cycloaltilisin 7 stood out with binding energies as low as −10.71 kcal/mol, indicating its robust inhibitory potential across multiple receptors. Similarly, Sitosterol showed consistent low binding energy values, especially −10.71 kcal/mol, positioning it as a promising candidate for enzyme inhibition. Artocarpin and Atocarpesin displayed moderate binding affinities, with binding energies

Table 2 Molecular Docking Simulations of Metabolites Identified in Artocarpus Heterophyllus Extracts on Fibroblast Collagenase, Elastase, MITF, MMP-1, and MMP-2 Predicted Potential Inhibitory Compounds

Prediction Compound	PDB ID: 1CGL	PDB ID: 3HGP	PDB ID: 5T3Q	PDB ID: 1HFC	PDB ID: 1HOV
	MMGBSA Binding Energy (kcal/mol)				
Artocarpin	−7.94	−8.02	−8.87	−8.49	−9.24
Atocarpesin	−7.75	−7.61	−8.72	−7.73	−9.32
Vanillylidene-acetone	−5.85	−5.19	−6.29	−5.83	−6.60
(2s)-2-[(4-{1-hydroxy-3-imino	−6.30	−6.73	−8.14	−6.09	−9.94
2s)-3-{[2-(4-hydroxyphenyl)acetyl]oxy}	−5.33	−5.09	−6.75	−5.93	−5.08
2-{[3-(4-hydroxyphenyl)prop	−4.64	−5.86	−6.13	−4.15	−4.48
Cintramide	−5.72	−4.87	−6.35	−6.33	−6.69
Artocarpanone-3	−7.13	−7.09	−8.04	−7.38	−8.16
Licoflavone C-1	−7.66	−7.03	−8.92	−8.19	−8.52
ethyl-felurate-9	−5.87	−5.14	−6.35	−6.06	−6.48
Cycloaltilisin 7 (6)	−8.30	−7.98	−10.19	−8.90	−9.56
3,4,5-trimethoxy-cinnamic-acid	−5.46	−4.58	−7.09	−5.89	−5.23
3-[4-(acetyloxy)phenyl]-7-methoxy	−7.43	−7.61	−8.86	−7.69	−8.88
2{[1,3-dihydroxy-1(4-hydroxy-3-methoxy	−4.50	−3.71	−4.36	−5.51	−3.97
Asterric acid	−4.13	−4.85	−5.78	−4.04	−5.61
[7-hydroxy-4-oxo-2-(2-oxopropyl)-2,3-dihydro-1-benzopyran-5-yl] acetic acid	−5.88	−6.74	−6.87	−5.88	−6.70
5,7-dihydroxy-2-(2-hydroxy-4,6-dimethoxyphenyl)-2,3-dihydro-1-benzopyran-4-one	−6.91	−7.03	−7.48	−7.84	−8.17
7-(2-hydroxyethoxy)-6-methoxychromen-2-one	−6.31	−5.42	−6.46	−6.81	−6.22
(6r)-9,11-dihydroxy-2,3,6-trimethoxy-8-(3-methylbut-2-en-1-yl)-6h-5,7-dioxatetraphen-12-one	−7.85	−7.08	−8.76	−8.08	−7.24
Sitosterol	−8.93	−7.48	−10.71	−8.46	−8.14

around −8.87 and −8.72 kcal/mol, suggesting potential effectiveness in enzyme inhibition. Other compounds, like Licoflavone C-1 and Artocarpanone-3, exhibited notable binding energies, implying they may contribute to inhibition, although with slightly weaker affinities than Cycloaltilisin 7 and Sitosterol. This diversity of binding affinities across compounds highlights the broad bioactive potential of *Artocarpus heterophyllus* extracts. The results suggest a promising foundation for further exploration of these compounds in enzyme inhibition applications.

Table 3 provides additional insights into the inhibitory potential of compounds from *Artocarpus heterophyllus* ethyl acetate and ethanol extracts, with Sitosterol and Cycloaltilisin 7 showing exceptional binding affinities. Sitosterol demonstrated the strongest interaction, with binding energies as low as −13.00 kcal/mol, highlighting its high affinity and potential as a powerful enzyme inhibitor. Cycloaltilisin 7 also maintained low binding energies across multiple targets, reaching −11.19 kcal/mol, which reinforces its inhibitory capability. Other compounds, such as Artocarpanone-3 and Licoflavone C-1, displayed binding energies of −9.88 and −10.62 kcal/mol, suggesting they could contribute to enzyme inhibition, although with slightly less potency. Compounds like (2s)-2-[(4-{1-hydroxy-3-imino) and 2-{3-(4-hydroxyphenyl)prop showed promising affinities with binding energies around −10.91 and −11.00 kcal/mol. However, Vanillylidene-acetone and Cintramide exhibited higher binding energies, indicating weaker interactions compared to other more effective compounds. The array of binding affinities observed in these compounds reflects the bioactive diversity within *Artocarpus heterophyllus* extracts. The findings reinforce the notion that certain compounds are better suited as enzyme inhibitors, based on their strong and stable predicted interactions.[45]

Considering the binding energy data, Artocarpin and Sitosterol were selected for further molecular dynamics (MD) simulations to assess their potential as enzyme inhibitors. Artocarpin showed moderate but consistent binding energies across various enzyme targets, suggesting it may retain effective inhibition even in dynamic biological conditions.

Table 3 Molecular Docking Simulations on MMP-8, MMP-9, MMP-13, TGF-Beta Receptor Type 1 Kinase, and Human Tyrosinase-Related Protein 1 to Identify Potential Inhibitory Compounds Within Artocarpus Heterophyllus Extracts

Prediction Compound	PDB ID: 5H8X	PDB ID: 2OW1	PDB ID: 2OZR	PDB ID: 6B8Y	PDB ID: 5M8Q
	MMGBSA Binding Energy (kcal/mol)				
Artocarpin	−5.99	−9.95	−10.98	−9.59	−6.65
Atocarpesin	−5.89	−10.74	−10.69	−8.77	−6.54
vanillylidene-acetone	−4.33	−6.75	−7.30	−5.82	−5.10
(2s)-2-[(4-{1-hydroxy-3-imino	−10.40	−10.91	−10.00	−8.05	−7.05
2s)-3-{[2-(4-hydroxyphenyl)acetyl]oxy}	−8.24	−6.27	−8.28	−5.29	−5.25
2-{[3-(4-hydroxyphenyl)prop	−11.00	−6.51	−8.52	−5.30	−4.52
Cintramide	−4.88	−6.78	−7.01	−6.05	−4.99
Artocarpanone-3	−5.54	−9.88	−9.08	−9.14	−6.05
Licoflavone C-1	−5.51	−9.22	−10.62	−8.05	−6.39
ethyl-felurate-9	−4.46	−6.80	−7.23	−5.92	−5.15
Cycloaltilisin 7 (6)	−6.79	−10.81	−11.19	−10.44	−8.19
3,4,5-trimethoxy-cinnamic-acid	−8.07	−5.57	−7.98	−5.38	−4.55
3-[4-(acetyloxy)phenyl]-7-methoxy	−6.39	−10.23	−10.22	−9.09	−7.27
2{[1,3-dihydroxy-1(4-hydroxy-3-methoxy	−3.52	−6.99	−7.27	−4.69	−3.58
Asterric acid	−8.10	−5.44	−7.15	−5.89	−4.69
[7-hydroxy-4-oxo-2-(2-oxopropyl)-2,3-dihydro-1-benzopyran-5-yl] acetic acid	−8.89	−7.71	−9.06	−6.75	−5.76
5,7-dihydroxy-2-(2-hydroxy-4,6-dimethoxyphenyl)-2,3-dihydro-1-benzopyran-4-one	−5.13	−8.81	−8.77	−8.57	−6.08
7-(2-hydroxyethoxy)-6-methoxychromen-2-one	−4.88	−7.36	−8.13	−5.92	−5.84
(6r)-9,11-dihydroxy-2,3,6-trimethoxy-8-(3-methylbut-2-en-1-yl)-6h-5,7-dioxatetraphen-12-one	−6.11	−8.20	−10.06	−8.03	−6.27
Sitosterol	−6.72	−12.36	−13.00	−9.94	−8.06

https://doi.org/10.2147/DDDT.S507658

Sitosterol, with its remarkably low binding energies, particularly −13.00 kcal/mol against MMP-13, demonstrated the strongest predicted interaction, marking it as an ideal candidate for MD simulations. This selection is further justified by Sitosterol's broad affinity across multiple targets, indicating versatility in enzyme inhibition. The strong and stable interactions of Artocarpin and Sitosterol suggest they are likely to maintain their binding under dynamic conditions, a crucial factor for effective inhibition in complex biological systems. By progressing to MD simulations, the inhibitory mechanisms of these compounds can be further elucidated. This approach will provide a deeper understanding of their behavior, stability, and effectiveness in enzyme inhibition.[46] Thus, Artocarpin and Sitosterol stand out as promising candidates for advanced studies, due to their stable and high-affinity interactions.

To deepen the analysis of Artocarpin and Sitosterol as inhibitors of MMP-13, Figure 3 also presents a detailed view of their molecular interactions within the enzyme's active site. Artocarpin exhibits strong binding through hydrogen bonds with key residues, such as TYR223, TYR225, and LEU197, along with pi-stacking interactions, which contribute to its stable positioning within the binding pocket. These interactions, especially the hydrogen bonds and hydrophobic contacts, indicate that Artocarpin can effectively engage MMP-13's active site, supporting its potential as an inhibitor.

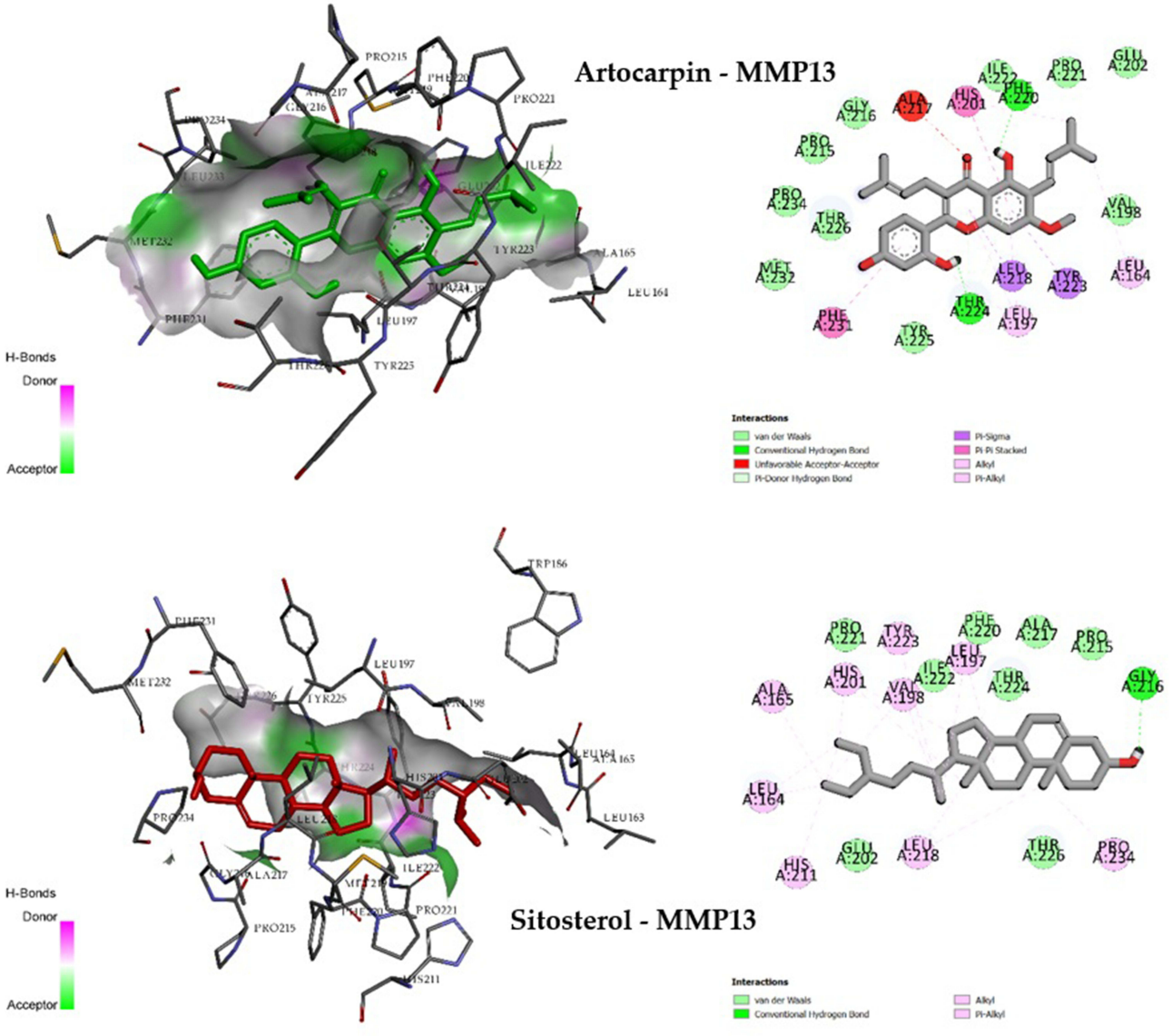

Figure 3 The molecular interactions of MMP-13 with Artocarpin and Sitosterol as predicted inhibitory compounds within *Artocarpus heterophyllus* extracts.

Sitosterol, on the other hand, shows an even stronger affinity for MMP-13, as evidenced by its low binding energy of −13.00 kcal/mol. This binding is reinforced through extensive hydrophobic interactions with residues like LEU163, LEU197, and MET232, as well as stabilizing hydrogen bonds involving ASP164 and TYR225. The range of interactions—hydrophobic, pi-alkyl, and hydrogen bonds—suggests that Sitosterol has a robust and versatile binding mode, allowing it to mimic natural substrate interactions effectively within the MMP-13 binding pocket. These stable interactions in both Artocarpin and Sitosterol complexes highlight their potential as inhibitors of MMP-13. This complex binding profile supports their selection for further molecular dynamics (MD) simulations to observe whether these interactions are maintained under dynamic conditions, validating their effectiveness in a biologically relevant setting.

Multi Targeted Molecular Dynamics Simulation

The molecular dynamics analysis of the Artocarpin complex system across various targets (Table 4), provides a comprehensive understanding of several key structural parameters, including gyration radius (Rg), radial distribution function (RDF), root mean square deviation (RMSD), root mean square fluctuation (RMSF), and solvent-accessible surface area (SASA). Rg was used to measure the compactness of each complex; for example, the MITF complex has the highest Rg value of 2.01 nm, indicating a relatively expanded structure, while MMP-8 has a more compact structure with a Rg value of 1.47 nm. The RDF values provide insight into the distribution of atoms around a central point, with the highest RDF observed in the MITF complex at 5.27, suggesting a distinctive molecular arrangement compared to other targets. RMSD, an indicator of complex stability, showed variation across complexes, where elastase displayed the lowest RMSD of 0.17 nm, indicating the greatest rigidity, while MMP-2 exhibited a higher RMSD of 0.48 nm, reflecting greater flexibility in the Artocarpin-MMP-2 complex. RMSF analysis highlights the flexibility of specific regions within each complex, with values ranging from 0.09 nm in elastase to 0.23 nm in MMP-8, showing that different targets have varying levels of residue mobility. The SASA values, which reflect the exposed surface area of each complex, ranged from 82.31 nm² in MMP-8 to 186.67 nm² in human tyrosinase-related protein 1, suggesting varying degrees of interaction with the solvent environment. These combined parameters reveal that each Artocarpin-protein complex displays distinct structural properties, which could influence their binding affinity and stability. These findings provide a foundation for further studies on Artocarpin's potential inhibitory effects, with the variability across parameters suggesting diverse functional behaviors in different protein targets.

The Sitosterol complex system similarly demonstrates a range of structural characteristics across various protein targets, as shown in Table 5. The gyration radius (Rg) indicates that human tyrosinase has the least compact structure with an Rg of 2.15 nm, while MMP-8 is the most compact at 1.44 nm. Radial distribution function (RDF) values, which highlight atomic distribution, vary across complexes, with MMP-13 showing the highest RDF at 5.62, indicating a unique arrangement. The RMSD values, representing stability, reveal that elastase is the most stable complex with an RMSD of 0.16 nm, while MMP-2 is more flexible at 0.66 nm. RMSF analysis of residue mobility shows that elastase has the least flexible regions (0.09 nm), whereas MMP-8 displays greater flexibility at 0.23 nm. Solvent-accessible surface area (SASA) values suggest different solvent interaction levels, ranging from 79.21 nm^2 in MMP-8 to 186.46

Table 4 Mean Values of Molecular Dynamics Parameters for the Artocarpin Complex System

Complex System	Gyrate (nm)	RDF	RMSD (nm)	RMSF (nm)	SASA (nm^2)
Fibroblast collagenase	1.560507	3.370593	0.276481	0.142653	96.42322
Elastase	1.560507	1.560507	0.167917	0.090061	109.3412
MITF	2.018756	5.270193	0.271299	0.152998	147.4793
MMP-1	1.505652	3.725128	0.244411	0.123287	86.34126
MMP-2	1.569247	4.969902	0.478198	0.19973	99.41641
MMP-8	1.479828	3.699292	0.505234	0.235439	82.31824
MMP-9	1.532801	3.914359	0.358861	0.14403	91.19502
MMP-13	1.540981	5.637951	0.500783	0.144942	98.78395
TGF-Beta receptor type 1 kinase	1.983174	4.747586	0.204336	0.104515	151.3391
Human tyrosinase-related protein 1	2.147809	2.91825	0.177228	0.095471	186.6735

https://doi.org/10.2147/DDDT.S507658

Table 5 Average Molecular Dynamics Parameter Values for the Sitosterol Complex System

Complex System	Gyrate (nm)	RDF	RMSD (nm)	RMSF (nm)	SASA (nm^2)
Fibroblast collagenase	1.5631343	3.474758	0.269405	0.136234	96.13048
Elastase	1.680967	2.888094	0.156821	0.08729	109.7904
MITF	2.073616	4.640837	0.350326	0.182518	149.1573
MMP-1	1.498124	3.204036	0.225802	0.117159	86.43791
MMP-2	1.641595	4.742191	0.658759	0.190224	104.7962
MMP-8	1.438876	3.953732	0.593154	0.235333	79.21125
MMP-9	1.523239	3.757496	0.337119	0.159566	91.19387
MMP-13	1.563113	5.623033	0.479599	0.160507	99.90046
TGF-Beta receptor type 1 kinase	1.985709	4.226182	0.182633	0.103267	149.7707
Human tyrosinase-related protein 1	2.145741	3.285609	1.154227	0.101151	186.463

nm^2 in human tyrosinase, reflecting varying degrees of structural openness. Together, these parameters underscore the unique structural profiles of each Sitosterol-protein complex, potentially affecting their binding dynamics and biological activity. This structural diversity highlights Sitosterol's versatile interactions, offering insights for future studies on its therapeutic potential across different protein targets.

The comparative molecular dynamics analysis between Artocarpin and Sitosterol complexes with MMP-2, as illustrated in the Figure 4, reveals notable differences in stability and structural flexibility. The RMSD values over time suggest that Artocarpin maintains a more stable binding to MMP-2, with consistently lower RMSD values compared to Sitosterol, which shows greater fluctuation throughout the simulation. This stability in Artocarpin is further supported by the Radius of Gyration (Rg) values, where Artocarpin exhibits a more compact structure, indicating that it holds a tighter conformation within the complex. In contrast, Sitosterol has higher and more variable Rg values, suggesting a less compact and potentially more adaptable interaction with MMP-2. Such differences in Rg values could imply that Sitosterol undergoes conformational changes more readily, affecting the overall structural integrity of the complex. This compactness in Artocarpin likely contributes to its stability, as a more rigid structure is often associated with stronger binding affinity. Additionally, these results suggest that Artocarpin may form a more robust interaction with MMP-2, which can be advantageous in applications that require stability. The contrasting behaviors observed in these RMSD and Rg values highlight the fundamental differences in how each compound interacts with MMP-2 on a structural level.

Moreover, the RMSF analysis provides insights into the residue-specific flexibility within each complex, further elucidating the dynamics of Artocarpin and Sitosterol with MMP-2. Artocarpin displays generally lower RMSF values across most residues, signifying less residue mobility and indicating a firmer binding interaction at specific regions of the protein. On the other hand, Sitosterol exhibits higher RMSF peaks at several residues, which implies localized flexibility that could influence its binding stability. Additionally, the SASA values show that Sitosterol maintains higher solvent accessibility, suggesting a more exposed binding configuration, while Artocarpin's lower SASA values indicate a more enclosed interaction with MMP-2. This greater exposure in Sitosterol may allow for more transient interactions with the surrounding environment but can also lead to reduced stability. Lastly, the RDF analysis reflects slight variations in atomic distribution, with Sitosterol showing a higher density at certain distances, indicative of unique structural arrangements within the binding site. Collectively, these findings suggest that Artocarpin's interaction with MMP-2 is characterized by enhanced stability and compactness, whereas Sitosterol displays a more flexible and open structure. These differences could significantly impact their respective binding dynamics, providing essential insights for potential therapeutic applications targeting MMP-2.

Molecular Mechanics-Poisson Boltzmann Surface Area (MM-PBSA) Calculations

The binding free energy represents the non-bonded interaction strength between Artocarpin and Sitosterol molecules and their target proteins. Calculated using the MM-PBSA method, the binding free energies offer insights into the varying affinities of these compounds for different biological targets. In the case of Artocarpin, each target protein displayed

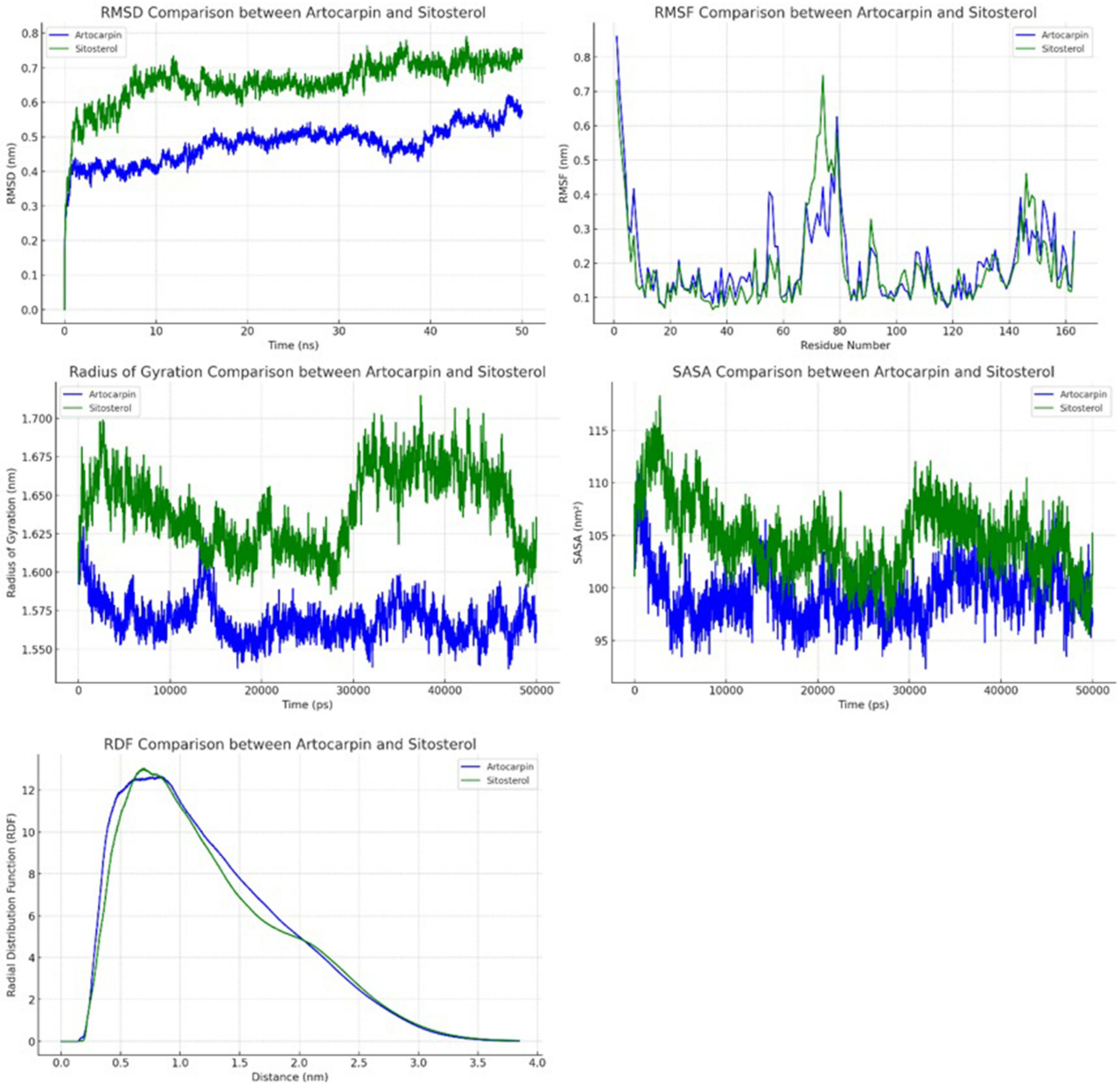

Figure 4 Comparative molecular dynamics analysis of Artocarpin and Sitosterol complexes with MMP-2.

a distinct $\Delta G_{MM/PBSA}$ value, reflecting its unique binding affinity (Table 6). The fibroblast collagenase complex, for instance, showed a binding energy of −62.04 kJ/mol, which suggests a moderate interaction strength. The elastase complex exhibited a slightly weaker binding, with an energy of −47.14 kJ/mol, indicating a lesser affinity compared to other targets. The MITF complex, however, demonstrated a stronger interaction with Artocarpin, with a binding free energy of −101.45 kJ/mol. Notably, Artocarpin's highest affinities were observed in complexes with MMP-13 and TGF-Beta receptor type 1 kinase, where the binding energies reached −131.51 kJ/mol and −118.52 kJ/mol, respectively. These findings suggest that Artocarpin has a strong binding preference for certain protein targets, which may hold significance for therapeutic applications targeting these specific proteins.

Similarly, the Sitosterol complexes displayed a range of binding free energies across different protein targets, highlighting its diverse interaction profile (Table 7). Analysis of Sitosterol's interactions revealed a moderately strong binding affinity with fibroblast collagenase, with a binding free energy of −88.24 kJ/mol. A similar energy was observed in the elastase complex, with a binding energy of −85.98 kJ/mol, showing a comparable level of affinity. The MITF

https://doi.org/10.2147/DDDT.S507658

Table 6 Computed Binding Free Energies of Artocarpin Complexes

Complex System	ΔG_{vdw} (kJ/mol)	ΔG_{elec} (kJ/mol)	ΔG_{polar} (kJ/mol)	ΔG_{surf} (kJ/mol)	$\Delta G_{MM/PBSA}$ (kJ/mol)
Fibroblast collagenase	−96.44	−46.774	93.145	−11.966	−62.035
Elastase	−85.725	−23.176	71.91	−10.144	−47.135
MITF	−169.527	−36.363	123.127	−18.688	−101.451
MMP-1	−159.363	−22.171	98.744	−16.069	−98.859
MMP-2	−128.755	−31.324	99.441	−12.072	−72.71
MMP-8	−101.044	−16.527	67.872	−11.62	−61.32
MMP-9	−179.521	−25.681	111.144	−16.306	−110.364
MMP-13	−217.104	−15.642	120.488	−19.246	−131.505
TGF-Beta receptor type 1 kinase	−203.719	−26.661	132.923	−21.065	−118.523
Human tyrosinase-related protein 1	−122.633	−42.466	107.456	−14.179	−71.822

complex, bound to Sitosterol, displayed a slightly stronger interaction with a binding energy of −90.70 kJ/mol. Interestingly, MMP-1 and MMP-8 also exhibited moderate affinities with Sitosterol, showing binding free energies of −86.67 kJ/mol and −83.81 kJ/mol, respectively. Among the Sitosterol complexes, the MMP-2 complex displayed the strongest binding affinity, with a significant energy of −167.80 kJ/mol, which suggests a particularly high affinity for this target. MMP-13 also showed a strong affinity for Sitosterol, with a binding free energy of −132.28 kJ/mol, indicating that Sitosterol has a high potential for interactions with matrix metalloproteinases.

The calculated binding energies highlight the specific affinities that Artocarpin and Sitosterol have for various protein targets, which could inform their potential applications in targeted therapies. Artocarpin shows notable affinity with MMP-13 and TGF-Beta receptor type 1 kinase, suggesting that it may be effective in modulating the activity of these proteins. In contrast, Sitosterol exhibits a pronounced binding affinity with MMP-2 and MMP-13, pointing to its potential role in influencing matrix metalloproteinase activity. The range of binding free energies in both compounds reflects the complexity and specificity of their interactions with biological targets. These affinities could be leveraged in drug development, where specific binding to target proteins is essential for therapeutic effectiveness. Additionally, the detailed breakdown of binding energies across different interaction types (including van der Waals, electrostatic) provides a comprehensive understanding of how these molecules interact with their targets at the molecular level.[47,48]

DPPH Radical Scavenging and Tyrosinase Enzyme Inhibitory Activities

The Figure 5 and Table 8 shows the antioxidant and tyrosinase enzyme inhibitory activities of different extracts from *Artocarpus heterophyllus* leaves, using ascorbic acid and kojic acid as standard references. The ethyl acetate extract demonstrated a higher antioxidant activity of 117.64 ppm compared to the ethanol extract, which had a lower activity of 56.50 ppm. When compared to ascorbic acid, which showed an antioxidant activity of 5.39 ppm, both extracts had much lower potency. This suggests that although the *Artocarpus heterophyllus* leaf extracts possess antioxidant properties, they

Table 7 Evaluated Binding Free Energies for Sitosterol Complexes

Complex System	ΔG_{vdw} (kJ/mol)	ΔG_{elec} (kJ/mol)	ΔG_{polar} (kJ/mol)	ΔG_{surf} (kJ/mol)	$\Delta G_{MM/PBSA}$ (kJ/mol)
Fibroblast collagenase	−113.276	−8.076	46.034	−12.927	−88.244
Elastase	−118.112	−2.273	48.75	−14.342	−85.977
MITF	−137.388	−10.302	73.292	−16.298	−90.696
MMP-1	−120.987	−31.134	78.163	−12.715	−86.673
MMP-2	−227.301	−2.648	84.531	−22.377	−167.795
MMP-8	−120.756	−6.386	57.267	−13.932	−83.807
MMP-9	−162.196	−10.056	72.636	−16.311	−115.927
MMP-13	−177.064	−6.572	68.161	−16.801	−132.275
TGF-Beta receptor type 1 kinase	−38.217	−1.19	13.1	−4.48	−30.786
Human tyrosinase-related protein 1	−138.485	−16.993	72.959	−15.345	−97.864

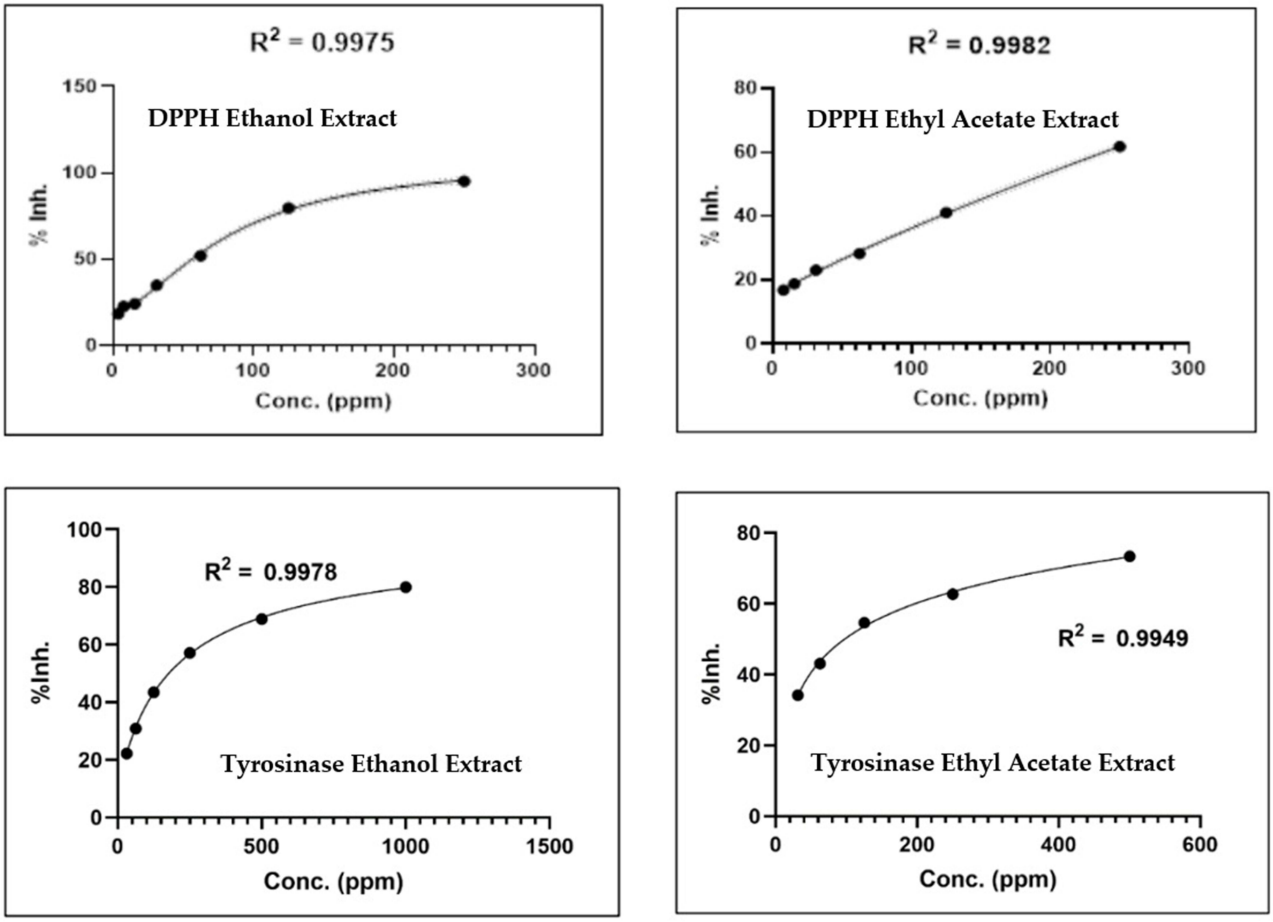

Figure 5 DPPH radical scavenging and tyrosinase inhibitory activities of *Artocarpus heterophyllus* leaf extracts.

are relatively weak antioxidants in comparison to ascorbic acid. Antioxidants play a crucial role in neutralizing free radicals, and the varying effectiveness of these extracts could be due to the different phytochemicals extracted by each solvent. Ethyl acetate, being a semi-polar solvent, might have extracted more antioxidant compounds, leading to its higher activity. The relatively low antioxidant activity of the ethanol extract suggests that it may contain fewer or less effective antioxidant compounds.[49,50] This variation highlights the influence of solvent choice on the types of compounds extracted and their resulting bioactivity.

In terms of tyrosinase enzyme inhibition, the ethanol extract displayed a significant inhibitory activity of 177.24 ppm, much higher than the ethyl acetate extract at 97.16 ppm. Both extracts outperformed kojic acid, a standard tyrosinase inhibitor, which had an activity of 45.96 ppm. Tyrosinase inhibition is essential in controlling melanin production, making these extracts valuable for cosmetic applications targeting skin pigmentation. The higher tyrosinase inhibition in the ethanol extract suggests that polar solvents may be more effective in extracting compounds that inhibit this enzyme.[51,52] Ethanol likely extracts more polar compounds with strong anti-tyrosinase properties, which contributes to its high inhibitory activity. The ethyl acetate extract, while also effective, may lack the potency of the ethanol extract in

Table 8 Antioxidant and Tyrosinase Enzyme Inhibitory Activities of Artocarpus Heterophyllus Leaf Extracts

Sample	Antioxidant Activity (ppm)	Tyrosinase Enzyme Inhibitory (ppm)
Comparison	5.39 (Ascorbic Acid)	45.96 (Kojic Acid)
Ethyl acetate extract of *Artocarpus heterophyllus* leaves	117.64	97.16
Ethanol extract of *Artocarpus heterophyllus* leaves	56.50	177.24

https://doi.org/10.2147/DDDT.S507658

this regard. These findings indicate that *Artocarpus heterophyllus* leaf extracts, especially when prepared with ethanol, could be promising natural alternatives for tyrosinase inhibition. Such properties make them potential candidates for use in skincare formulations aimed at reducing hyperpigmentation and promoting even skin tone.

Discussion

The study on *Artocarpus heterophyllus* leaf extracts, with a focus on the compounds Artocarpin and Sitosterol, reveals considerable bioactive potential, particularly in pharmaceutical and cosmetic contexts. Using ethyl acetate and ethanol as extraction solvents, a range of bioactive compounds were isolated, notably including flavonoids and terpenoids/steroids. LC-MS/MS analysis further identified dominant compounds such as Cintramide and Licoflavone C in the ethyl acetate extract, while the ethanol extract exhibited a more diverse composition, including (2S)-2-[(4-{1-hydroxy-3-imino}phenyl) formamido]pentanedioic acid and additional phenolic acids. These findings underscore the complementarity of extraction methods in isolating distinct phytochemical profiles. Ethanol extraction proved especially effective, yielding a more diverse profile of bioactive compounds, including phenolic acids, which are essential in managing oxidative stress. Artocarpin, one of the primary compounds identified in the ethanol extract, and Sitosterol, found in lower concentrations in the ethyl acetate extract, are key contributors to the therapeutic value of the extract. Artocarpin's recognized antioxidant and anti-inflammatory properties support its potential in pharmaceutical applications targeting inflammatory and oxidative stress-related diseases.[53,54] Meanwhile, Sitosterol's structural qualities position it as an ideal candidate for enzyme inhibition.[55] This solvent-selective approach highlights how extraction methods influence bioactive composition, guiding targeted extraction of specific therapeutic compounds. By focusing on Artocarpin and Sitosterol, the study demonstrates how *Artocarpus heterophyllus* leaf extracts may serve as a source of valuable compounds for health applications.

Molecular docking simulations further emphasized the enzyme inhibition potential of Artocarpin and Sitosterol, showing their strong binding affinities with enzymes such as MMP-1, MMP-2, and MMP-13. These enzymes are key players in tissue remodeling and inflammation, processes often overactive in chronic inflammatory conditions and certain cancers. Sitosterol's notably low binding energy with MMP-13 suggests a stable interaction, positioning it as a potent inhibitor with potential to disrupt MMP-related pathological pathways. Artocarpin, though slightly less potent than Sitosterol, still displayed significant binding affinity with MMP enzymes, indicating that it could modulate enzyme activity in diseases involving excessive MMP activity, such as chronic inflammation, arthritis, and cancer metastasis. To verify these initial findings, molecular dynamics (MD) simulations were conducted, providing a more comprehensive picture of how Artocarpin and Sitosterol behave over time when bound to their targets. Low Root Mean Square Deviation (RMSD) values for Artocarpin suggest a stable interaction with MMPs, as minimal structural deviation implies a steady binding. Additionally, both compounds exhibited low Radius of Gyration (Rg) values, indicating compact binding conformations essential for effective enzyme inhibition.[56] The MD results, therefore, reinforce the potential of Artocarpin and Sitosterol as stable, natural MMP inhibitors, laying a foundation for their further exploration as therapeutic agents.

Beyond enzyme inhibition, the antioxidant and tyrosinase inhibitory activities of Artocarpin and Sitosterol offer additional therapeutic and cosmetic benefits. Artocarpin, particularly in the ethanol extract, displayed significant antioxidant activity, effectively scavenging free radicals, though slightly less potent than ascorbic acid. This antioxidant capacity suggests its utility in managing oxidative stress, a contributing factor in numerous chronic conditions, including aging-related diseases and cancer. Sitosterol, on the other hand, exhibited impressive tyrosinase inhibition, even outperforming kojic acid—a standard tyrosinase inhibitor widely used in cosmetic applications. Tyrosinase inhibition is crucial for managing melanin production and hyperpigmentation, making Sitosterol valuable for formulations aimed at achieving even skin tone. The polar nature of ethanol likely enhanced the extraction of tyrosinase-inhibiting compounds, making the ethanol extract particularly promising for pigmentation control in cosmetic applications.[57,58] These results underscore the versatility of Artocarpin and Sitosterol, suggesting that they could be used in both skincare and health products. For Artocarpin, studies have shown limited solubility in aqueous environments, with an estimated bioavailability of less than 20%, which may restrict its effectiveness unless advanced delivery systems such as nanoparticles or encapsulation are applied to enhance its absorption. Sitosterol, on the other hand, demonstrates moderate bioavailability, typically ranging between 30% and 40% in oral formulations, though its hydrophobic nature necessitates solubilization

techniques to improve systemic uptake. Addressing these bioavailability challenges is essential to maximize their therapeutic and cosmetic potential, paving the way for their incorporation into innovative and effective formulations.

Additionally, in vivo studies are essential to evaluate the impact of Artocarpin and Sitosterol under physiological conditions, focusing on oxidative stress mitigation, enzyme inhibition, melanin regulation, and anti-inflammatory effects. Advanced formulation strategies, such as nanoemulsions or liposomal delivery systems, could significantly enhance the bioavailability and stability of these compounds, ensuring prolonged activity and precise delivery to target sites. These technologies can also reduce potential side effects by minimizing off-target interactions, which is critical for their application in pharmaceutical and cosmetic products.[59,60] The ability to combine these advanced formulations with natural bioactive compounds like Artocarpin and Sitosterol offers a promising avenue for creating more effective treatments. Furthermore, validating these compounds through clinical trials will provide definitive evidence of their therapeutic and cosmetic potential, especially in addressing age-related conditions, pigmentation disorders, and inflammatory diseases. Ultimately, this study lays the groundwork for leveraging *Artocarpus heterophyllus* leaf extracts in modern health and skincare solutions.

Conclusion

In conclusion, this study highlights the significant bioactive potential of *Artocarpus heterophyllus* leaf extracts for therapeutic and cosmetic applications. Artocarpin and Sitosterol, the primary bioactive compounds identified, exhibit notable antioxidant and tyrosinase inhibition activities. Ethanol extracts demonstrated stronger tyrosinase inhibition with an IC_{50} value of 177.24 ppm, while ethyl acetate extracts showed superior antioxidant activity with an IC_{50} value of 117.64 ppm. Molecular docking and molecular dynamics (MD) simulations further validated the potential of these compounds, with Artocarpin showing stable binding interactions with MMP-13, underscoring its role as a therapeutic agent targeting enzyme inhibition. These findings reveal the potential of *Artocarpus heterophyllus* leaf extracts in addressing oxidative stress, inflammation, and hyperpigmentation-related disorders. Future research should focus on conducting comprehensive in vivo studies to confirm these bioactivities under physiological conditions and optimizing advanced delivery systems, such as nanoemulsions or liposomal formulations, to enhance the bioavailability and stability of these compounds. By integrating these approaches, *Artocarpus heterophyllus* leaf extracts could pave the way for innovative plant-based solutions in modern therapeutic and cosmetic applications.

Acknowledgments

This work was supported by a grant from the Ministry of Education, Culture, Research, and Technology (Kemendikbudristek) of Indonesia under Contract Number: 305/B.04/Rek/VI/2024. We extend our gratitude for their funding and support, which made this research possible.

Disclosure

Dr. Lelly Yuniarti, S.Si., M.Kes; Dr. Maya Tejasari, dr., M.Kes; Dr. R. Anita Indriyanti, dr., M.Kes; and apt. Taufik Muhammad Fakih, S.Farm., M.S.Farm report a patent "Optimization of Extraction and Identification Protocols for Bioactive Compounds in Jackfruit Leaves (Artocarpus heterophyllus) Utilizing High-Resolution Liquid Chromatography Mass Spectrometry (LC-HRMS) for Anti-Aging Application [S00202410299]" issued. The authors declare no other conflicts of interest regarding the publication of this article.

References

1. Wang Y, Li J, Xia L. Plant-derived natural products and combination therapy in liver cancer. *Front Oncol*. 2023;13. doi:10.3389/fonc.2023.1116532
2. Atanasov AG, Waltenberger B, Pferschy-Wenzig EM, et al. Discovery and resupply of pharmacologically active plant-derived natural products: a review. *Biotechnol Adv*. 2015;33(8):1582–1614. doi:10.1016/j.biotechadv.2015.08.001
3. Nisa RU, Nisa AU, Tantray AY, et al. Plant phenolics with promising therapeutic applications against skin disorders: a mechanistic review. *J Agric Food Res*. 2024;16. doi:10.1016/j.jafr.2024.101090
4. Cosme P, Rodríguez AB, Espino J, Garrido M. Plant phenolics: bioavailability as a key determinant of their potential health-promoting applications. *Antioxidants*. 2020;9(12):1263. doi:10.3390/antiox9121263
5. Gorzynik-Debicka M, Przychodzen P, Cappello F, et al. Potential health benefits of olive oil and plant polyphenols. *Int J mol Sci*. 2018;19(3):686. doi:10.3390/ijms19030686

6. Pandey KB, Rizvi SI. Plant polyphenols as dietary antioxidants in human health and disease. *Oxid Med Cell Longev*. 2009;2(5):270–278. doi:10.4161/oxim.2.5.9498
7. Salehi B, Azzini E, Zucca P, et al. Plant-derived bioactives and oxidative stress-related disorders: a key trend towards healthy aging and longevity promotion. *Appl Sci*. 2020;10(3):947. doi:10.3390/app10030947
8. Ranasinghe RASN, Maduwanthi SDT, Marapana RAUJ. Nutritional and health benefits of jackfruit (*Artocarpus heterophyllus* Lam.): a review. *Int J Food Sci*. 2019;2019:1–12. doi:10.1155/2019/4327183
9. Chhotaray S, Priyadarshini B. Nutritional composition and health benefits of jackfruit seed flour: a review. ~ *454* ~ *Pharma Innov J*. 2022;11(10): 42–49.
10. Afotey B, Yuorkuu E, Akinie S, Eshun F, Sufyan M. Determination of health and nutritional benefits of jackfruits (*Artocarpus heterophyllus*). *J Ghana Inst Eng*. 2024;24(1). doi:10.56049/jghie.v24i1.149
11. Saha S, Sarker M, Redwan Haque A, Ahmed Nayeem T, Rashed Maukeeb A. Asian Journal of Advances in Research A REVIEW ON TROPICAL FRUIT: JACKFRUIT (*Artocarpus heterophyllus*). *Asian J Adv Res*. 2022;5(1): 298–307.
12. Nansereko S, Muyonga JH. Exploring the potential of jackfruit(*Artocarpus heterophyllus* Lam). *Asian Food Sci J*. 2021;97–117. doi:10.9734/afsj/2021/v20i930346
13. Gupta A, Marquess AR, Pandey AK, Bishayee A. Jackfruit (*Artocarpus heterophyllus* Lam.) in health and disease: a critical review. *Crit Rev Food Sci Nutr*. 2023;63(23):6344–6378. doi:10.1080/10408398.2022.2031094
14. De Almeida AJPO, De Almeida Rezende MS, Dantas SH, et al. Unveiling the role of inflammation and oxidative stress on age-related cardiovascular diseases. *Oxid Med Cell Longev*. 2020;2020:1–20. doi:10.1155/2020/1954398
15. Vidyalakshmi S, Sahithya D. Preliminary screening of selected plant extracts for anti tyrosinase activity. *J Nat Remedies*. 2016;16(1). doi:10.18311/jnr/2016/488
16. Widelski J, Gaweł-Bęben K, Czech K, et al. Extracts from European Propolises as Potent Tyrosinase Inhibitors. *Molecules*. 2023;28(1). doi:10.3390/molecules28010055
17. Mandhare A, Banerjee P, Pande A, Gondkar A. Jackfruit (*Artocarpus heterophyllus*): a Comprehensive Patent Review. *Curr Nutr Food Sci*. 2019;16(5). doi:10.2174/1573401315666190730120759
18. Sandhya Rani S, Vedavijaya T, Sree PK, et al. A comprehensive analysis of phytochemical composition, acute toxicity assessment, and antioxidant potential of ethanolic extract of carica papaya seeds. *Cureus*. 2023. doi:10.7759/cureus.49686
19. Singh A, Mathur M, Pal Singh G. Phytochemical screening and Thin layer chromatographic identification of Terpenoids from the root extract of Achyranthes aspera l.- An Indian Ethanomedicine. *Int J Sci Res Publ*. 2016;6(6): 411–414.
20. Skorek M, Jurczyk K, Sajewicz M, Kowalska T. Thin-layer chromatographic identification of flavonoids and phenolic acids contained in cosmetic raw materials. *J Liq Chromatogr Relat Technol*. 2016;39(5–6):286–291. doi:10.1080/10826076.2016.1163467
21. Soraya S, Sukara E, Sinaga E. Identification of Chemical Compounds in Ziziphus mauritiana Fruit Juice by GC-MS and LC-MS/MS Analysis. *Int J Biol Phys Chem Stud*. 2022;4(2):11–19. doi:10.32996/ijbpcs.2022.4.2.2
22. Zhang L, Wang J, Li T, et al. Determination of the chemical components and phospholipids of velvet antler using UPLC/QTOF-MS coupled with UNIFI software. *Exp Ther Med*. 2019. doi:10.3892/etm.2019.7372
23. Tamada T, Kinoshita T, Kurihara K, et al. Combined high-resolution neutron and X-ray analysis of inhibited elastase confirms the active-site oxyanion hole but rules against a low-barrier hydrogen bond. *J Am Chem Soc*. 2009;131(31):11033–11040. doi:10.1021/ja9028846
24. Borkakot N, Winkler FK, Williams DH, et al. Structure of the catalytic domain of human fibroblast collagenase complexed with an inhibitor. *Nat Struct Biol*. 1994;1(2). doi:10.1038/nsb0294-106
25. Harikrishnan LS, Warrier J, Tebben AJ, et al. Heterobicyclic inhibitors of transforming growth factor beta receptor I (TGFβRI). *Bioorg Med Chem*. 2018;26(5):1026–1034. doi:10.1016/j.bmc.2018.01.014
26. Johnson AR, Pavlovsky AG, Ortwine DF, et al. Discovery and characterization of a novel inhibitor of matrix metalloprotease-13 that reduces cartilage damage in vivo without joint fibroplasia side effects. *J Biol Chem*. 2007;282(38):27781–27791. doi:10.1074/jbc.M703286200
27. Tochowicz A, Maskos K, Huber R, et al. Crystal structures of MMP-9 complexes with five inhibitors: contribution of the flexible Arg424 side-chain to selectivity. *J mol Biol*. 2007;371(4):989–1006. doi:10.1016/j.jmb.2007.05.068
28. Tauro M, Laghezza A, Loiodice F, et al. Catechol-based matrix metalloproteinase inhibitors with additional antioxidative activity. *J Enzyme Inhib Med Chem*. 2016;31(1):31. doi:10.1080/14756366.2016.1217853
29. Feng Y, Likos JJ, Zhu L, et al. Solution structure and backbone dynamics of the catalytic domain of matrix metalloproteinase-2 complexed with a hydroxamic acid inhibitor. *Biochim Biophys Acta - Protein Struct Mol Enzymol*. 2002;1598(1–2). doi:10.1016/s0167-4838(02)00307-2
30. Spurlino JC, Smallwood AM, Carlton DD, et al. 1.56 Å structure of mature truncated human fibroblast collagenase. *Proteins Struct Funct Bioinforma*. 1994;19(2):98–109. doi:10.1002/prot.340190203
31. Lai X, Wichers HJ, Soler-Lopez M, Dijkstra BW. Structure of Human Tyrosinase Related Protein 1 Reveals a Binuclear Zinc Active Site Important for Melanogenesis. *Angew Chem Int Educ*. 2017;56(33):9812–9815. doi:10.1002/anie.201704616
32. Schrödinger. Maestro | schrödinger. *Schrödinger Release 2018-1*. 2018.
33. Sonibare K, Rathnayaka L, Zhang L. Comparison of CHARMM and OPLS-aa forcefield predictions for components in one model asphalt mixture. *Constr Build Mater*. 2020;236. doi:10.1016/j.conbuildmat.2019.117577
34. Kotni Meena NC. QM/MM docking strategy and prime/MM-GBSA calculation of celecoxib analogues as N-myristoyltransferase inhibitors. *Virol Mycol*. 2015;04(01). doi:10.4172/2161-0517.1000141
35. Abraham MJ, Murtola T, Schulz R, et al. GROMACS: high performance molecular simulations through multi-level parallelism from laptops to supercomputers. *SoftwareX*. 2015;1-2:19–25. doi:10.1016/j.softx.2015.06.001
36. Van Der Spoel D, Lindahl E, Hess B, Groenhof G, Mark AE, Berendsen HJC. GROMACS: fast, flexible, and free. *J Comput Chem*. 2005;26 (16):1701–1718. doi:10.1002/jcc.20291
37. Huang J, Rauscher S, Nawrocki G, et al. CHARMM36m: an improved force field for folded and intrinsically disordered proteins. *Nat Methods*. 2016;14(1):71–73. doi:10.1038/nmeth.4067
38. Kumari R, Kumar R, Consortium OSDD, Lynn A. g_mmpbsa —A GROMACS Tool for High-Throughput MM-PBSA Calculations. *J Chem Inf Model*. 2014;54(7):1951–1962. doi:10.1021/ci500020m

39. Sirivibulkovit K, Nouanthavong S, Sameenoi Y. Paper-based DPPH assay for antioxidant activity analysis. *Anal Sci*. 2018;34(7):795–800. doi:10.2116/analsci.18P014
40. Garcia-Molina P, Garcia-Molina F, Teruel-Puche JA, Rodriguez-Lopez JN, Garcia-Canovas F, Muñoz-Muñoz JL. The relationship between the IC50 values and the apparent inhibition constant in the study of inhibitors of tyrosinase diphenolase activity helps confirm the mechanism of inhibition. *Molecules*. 2022;27(10):3141. doi:10.3390/molecules27103141
41. Shahwar D, Raza MA. Antioxidant potential of phenolic extracts of Mimusops elengi. *Asian Pac J Trop Biomed*. 2012;2(7):547–550. doi:10.1016/S2221-1691(12)60094-X
42. Quesada-Romero L, Fernández-Galleguillos C, Bergmann J, et al. Phenolic fingerprinting, antioxidant, and deterrent potentials of persicaria maculosa extracts. *Molecules*. 2020;25(13):3054. doi:10.3390/molecules25133054
43. Pereira-Coelho M, Haas IC, da S, et al. A green analytical method for the determination of polyphenols in wine by dispersive pipette extraction and LC-MS/MS. *Food Chem*. 2023;405. doi:10.1016/j.foodchem.2022.134860.
44. Ercan L, Doğru M. Determination of phenolic compounds in Nasturtium Officinale by LC-MS / MS using different extraction methods and different solvents. *Int J Chem Technol*. 2023;7(2):124–130. doi:10.32571/ijct.1150482
45. Hikmawati D, Fakih TM, Sutedja E, Dwiyana RF, Atik N, Ramadhan DSF. Pharmacophore-guided virtual screening and dynamic simulation of Kallikrein-5 inhibitor: discovery of potential molecules for rosacea therapy. *Informatics Med Unlocked*. 2022;28. doi:10.1016/j.imu.2022.100844
46. Zikri AT, Pranowo HD, Haryadi W. Stability, hydrogen bond occupancy analysis and binding free energy calculation from flavonol docked in DAPK1 active site using molecular dynamic simulation approaches. *Indones J Chem*. 2021;21(2). doi:10.22146/ijc.56087
47. Mishra A, Mulpuru V, Mishra N. Exploring the mechanism of action of podophyllotoxin derivatives through molecular docking, molecular dynamics simulation and MM/PBSA studies. *J Biomol Struct Dyn*. 2022. doi:10.1080/07391102.2022.2138549
48. Suwendar S, Jantan I, Fakih TM, et al. Structural basis for the recognition of anthelmintic activity of bioactive metabolite in watery rose apple leaf through in silico investigation. *J Biomol Struct Dyn*. 2023;43(3):1539–1551. doi:10.1080/07391102.2023.2292294
49. Waszkowiak K, Gliszczyńska-świgło A. Binary ethanol–water solvents affect phenolic profile and antioxidant capacity of flaxseed extracts. *Eur Food Res Technol*. 2016;242(5):777–786. doi:10.1007/s00217-015-2585-9
50. Sun C, Wu Z, Wang Z, Zhang H. Effect of ethanol/water solvents on phenolic profiles and antioxidant properties of Beijing propolis extracts. *Evid Based Complement Altern Med*. 2015;2015:1–9. doi:10.1155/2015/595393
51. Kabadayı SN, Sadiq N, Bin Hamayun M, Park N Il, Kim HY. Impact of sodium silicate supplemented, IR-treated panax ginseng on extraction optimization for enhanced anti-tyrosinase and antioxidant activity: a Response Surface Methodology (RSM) approach. *Antioxidants*. 2024;13(1). doi:10.3390/antiox13010054
52. Fan ZL, Li L, Bai XL, et al. Extraction optimization, antioxidant activity, and tyrosinase inhibitory capacity of polyphenols from Lonicera japonica. *Food Sci Nutr*. 2019;7(5):1786–1794. doi:10.1002/fsn3.1021
53. Wong SK, Tangah J, Chan HT, Chan EWC. Chemistry and pharmacology of artocarpin: an isoprenyl flavone from Artocarpus species. *Syst Rev Pharm*. 2018;9(1). doi:10.5530/srp.2018.1.12
54. Daud NN, Septama A, Simbak N, Rahmi E. The phytochemical and pharmacological properties of artocarpin from *Artocarpus heterophyllus*. *Asian Pac J Trop Med*. 2020;13(1). doi:10.4103/1995-7645.273567
55. Khan Z, Nath N, Rauf A, et al. Multifunctional roles and pharmacological potential of β-sitosterol: emerging evidence toward clinical applications. *Chem Biol Interact*. 2022;365:110117. doi:10.1016/j.cbi.2022.110117
56. Nurisyah, Ramadhan DSF, Dewi R, et al. Targeting EGFR allosteric site with marine-natural products of Clathria Sp.: a computational approach. *Curr Res Struct Biol*. 2024;7. doi:10.1016/j.crstbi.2024.100125
57. Obaid RJ, Mughal EU, Naeem N, et al. Natural and synthetic flavonoid derivatives as new potential tyrosinase inhibitors: a systematic review. *RSC Adv*. 2021;11(36):22159–22198. doi:10.1039/d1ra03196a
58. Panzella L, Napolitano A. Natural and bioinspired phenolic compounds as tyrosinase inhibitors for the treatment of skin hyperpigmentation: recent advances. *Cosmetics*. 2019;6(4):57. doi:10.3390/cosmetics6040057
59. Catalano A, Mitri K, Perugini P, Condrò G, Sands C. In vitro and in vivo efficacy of a cosmetic product formulated with new lipid particles for the treatment of aged skin. *J Cosmet Dermatol*. 2023;22(12):3329–3339. doi:10.1111/jocd.16016
60. Westman M, Al-Bader T, Merinville E, et al. In vivo cosmetic product efficacy testing by analyzing epidermal proteins extracted from tape strips. *Cosmetics*. 2014;1(1):29–36. doi:10.3390/cosmetics1010029